

A link between prompt optical and prompt γ -ray emission in γ -ray bursts

W. T. Vestrand¹, P. R. Wozniak¹, J. A. Wren¹, E. E. Fenimore¹, T. Sakamoto², R. R. White¹, D. Casperson¹, H. Davis¹, S. Evans¹, M. Galassi¹, K. E. McGowan¹, J. A. Schier³, J. W. Asa³, S. D. Barthelmy², J. R. Cummings², N. Gehrels², D. Hullinger², H. A. Krimm², C. B. Markwardt², K. McLean¹, D. Palmer¹, A. Parsons² & J. Tueller²

¹Los Alamos National Laboratory, Space Science and Applications Group, ISR-1, MS-D466, Los Alamos, New Mexico 87545, USA

²NASA Goddard Space Flight Center, Code 661, Greenbelt, Maryland 20771, USA

³The Pilot Group, 128 West Walnut Avenue, Unit C, Monrovia, California 91016, USA

The prompt optical emission that arrives with the γ -rays from a cosmic γ -ray burst (GRB) is a signature of the engine powering the burst, the properties of the ultra-relativistic ejecta of the explosion, and the ejecta's interactions with the surroundings^{1–5}. Until now, only GRB 990123 had been detected⁶ at optical wavelengths during the burst phase. Its prompt optical emission was variable and uncorrelated with the prompt γ -ray emission, suggesting that the optical emission was generated by a reverse shock arising from the ejecta's collision with surrounding material. Here we report prompt optical emission from GRB 041219a. It is variable and correlated with the prompt γ -rays, indicating a common origin for the optical light and the γ -rays. Within the context of the standard fireball model of GRBs, we attribute this new optical component to internal shocks driven into the burst ejecta by variations of the inner engine. The correlated optical emission is a direct probe of the jet isolated from the medium. The timing of the uncorrelated optical emission is strongly dependent on the nature of the medium.

Starting on 19 December 2004 at 01:42:18 UT, high-energy emission from a bright and very long duration γ -ray burst, named GRB 041219a, was measured by both the IBIS ('imager on board the INTEGRAL satellite') detector of the INTEGRAL satellite⁷ and the Burst Alert Telescope (BAT) of the Swift satellite⁸. The 15–350-keV fluence measured by the Swift BAT was approximately 1.55×10^{-4} erg cm⁻², placing it among the top few per cent of the 1,637 GRB events listed in the comprehensive fourth BATSE (Burst and Transient Source Experiment) catalogue⁹. The duration of γ -ray emission from GRB 041219a was approximately 520 s, making it one of the longest ever measured.

One of our RAPTOR ('rapid telescopes for optical response') telescopes¹⁰ began optical imaging of the GRB 041219a region at 01:44:13 UT, just 8 s after receipt of the INTEGRAL alert. The long duration of the burst allowed RAPTOR-S to measure the optical emission in a series of 30-s images for an unprecedented 6.4 min while prompt γ -rays were being emitted. At the location of an infrared transient identified¹¹ in subsequent images (starting at 01:49:18 UT) taken by the PAIRITEL telescope, our images show an earlier flash of optical emission (see Fig. 1) temporally coincident with the main γ -ray pulses. At its peak, the optical flash reached a measured R_c -band magnitude of $R_c = 18.6 \pm 0.1$ mag. However, the location of the event placed it in the Galactic plane and in a direction with high optical extinction (Galactic longitude and latitude: $l = 120^\circ$, $b = +0.1^\circ$). Using standard extinction maps¹², we estimate an R -band extinction of ~ 4.9 mag, but the true extinction may be larger¹³. Correcting for the nominal extinction, the peak flux we measured corresponds to a peak optical magnitude of $R_c \approx 13.7$ mag. (Error analysis and our transformation of unfiltered instrumental magnitudes to standard R_c -band

magnitudes employing standard stars¹⁴ are discussed in Supplementary Information.)

Light curves for prompt optical emission and prompt γ -ray emission from GRB 041219a are shown in Fig. 2a. The optical light curve shows: the onset of an optical flash as the dominant first γ -ray pulse begins, peak brightness during the first γ -ray pulse, continued optical emission during the secondary γ -ray peak, and a decay of the optical emission to below our detection threshold during the tertiary γ -ray enhancement.

Optical emission has been detected during the interval of prompt γ -ray emission only once before⁶, for GRB 990123. Except for an overall temporal scaling factor—GRB 041219a was about 6 times longer—the temporal morphology of the two γ -ray light curves is remarkably similar (Fig. 2). Like GRB 041219a, the γ -ray light curve for GRB 990123 had a precursor followed by a much larger primary pulse, a secondary pulse, and a smaller-amplitude tertiary flux enhancement composed of minor pulses. But in contrast to GRB 041219a, the optical light curve from GRB 990123 was low during the primary γ -ray pulse and, though more sparsely sampled, reached peak brightness after the second major pulse. This anti-correlation suggests that prompt optical emission from GRB 990123 was generated by a different process from the prompt γ -rays. The consensus interpretation is that the delayed optical peak is generated by a reverse shock^{13,15}, an interpretation supported by detections of the predicted rise to a peak radio flux about one day after the burst¹⁶.

For GRB 041219a, we find that the observed optical light curve is well fitted by assuming that the generation of prompt optical emission is correlated with the generation of prompt γ -ray

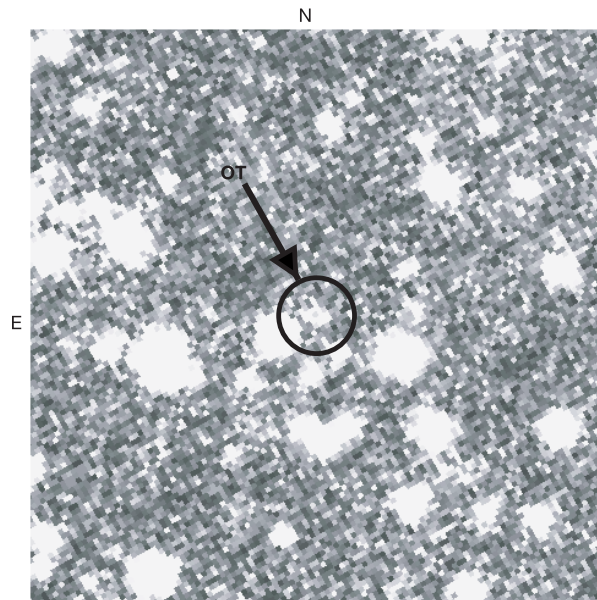


Figure 1 The prompt optical emission detected from GRB 041219a. This finder chart shows the location (right ascension 00 h 24 min 27.7 s, declination $+62^\circ 50' 33.5''$ (J2000)) of the prompt optical flash that we detected, simultaneously with the prompt γ -ray emission detected by the INTEGRAL⁷ and Swift⁸ satellites, during the time interval 01:45:41–01:49:01 UT on 2004 December 19. The location of the optical transient (OT) is identical to that found both for the subsequent infrared transient¹¹ and the optical counterpart²⁹ measured later during the late afterglow phase. Our observations of the prompt optical emission were obtained by RAPTOR-S, a 0.4-m, $f/5$, fully autonomous rapid response telescope owned by Los Alamos National Laboratory and located at an altitude of 2,500 m in the Jemez Mountains of New Mexico. The CCD camera employed for those observations has a $1,056 \times 1,027$ pixel format, back-illuminated, Marconi CCD47-10 chip with 13- μ m pixels.

emission. By integrating the observed 15–350-keV flux measured by Swift during the optical exposure intervals and multiplying by a derived constant optical to high-energy flux ratio, we predicted the optical light curve expected if the optical emission and γ -ray emission were perfectly correlated. As shown by the circles in Fig. 3, this simple constant-flux-ratio assumption predicts both the fast rise of the prompt optical emission observed at the start of the primary γ -ray pulse and the rapid decline observed after that dominant pulse. Our derived R_c -band optical to γ -ray flux logarithmic colour ratio for GRB 041219a is $(R_c - \gamma) = -2.5$ $\log(F_{\text{opt}}/F_\gamma) = 17.2$ or, after correcting for an R-band extinction of 4.9 mag, $(R_c - \gamma) = 12.3$.

The fast rise of optical emission simultaneous with the dominant γ -ray pulse, and a general correlation with the prompt γ -ray emission would naturally arise if emission in both energy bands

was generated by a common mechanism. The broadband spectra measured during the optical observation intervals are shown in Fig. 4. Modelling of the observed spectra is beyond the scope of this Letter, but it could distinguish between emission mechanisms and provide important constraints on physical conditions in the emitting region. A particularly attractive possibility, within the standard internal–external model for GRB fireballs, is that the prompt optical emission observed in GRB 041219a is a low-energy tail of the synchrotron emission¹⁷ generated by internal shocks in the GRB outflow². In that model, a nearly constant optical to γ -ray flux ratio requires cooling times short compared to the expansion time, and therefore magnetic fields near equipartition in the ejecta. However, possibilities exist for the emission mechanism—including, for example, saturated comptonization, which can generate correlated optical and γ -ray emission¹⁸.

Internal shock models² typically predict fainter prompt optical emission than do reverse shock models. Using the γ -ray fluxes measured for GRB 990123 and scaling by 1.2×10^{-5} (from the $(R_c - \gamma)$ colour derived for GRB 041219a), we predict significantly lower optical fluxes than measured in GRB 990123—except for the first point in the optical light curve. That first optical measurement, which occurred during the dominant γ -ray pulse, is consistent, within the prediction uncertainty, with the value predicted for an internal shock using the $(R_c - \gamma)$ colour for GRB 041219a. But after

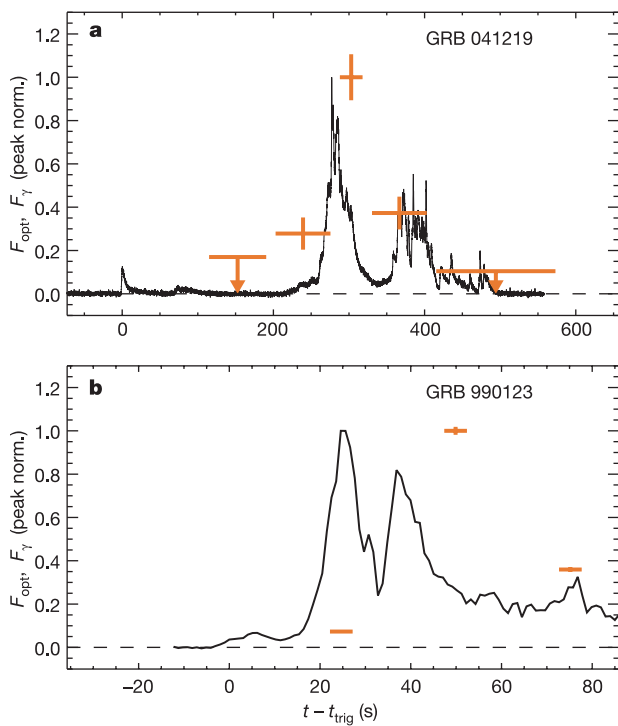


Figure 2 Comparison of the prompt γ -ray and prompt optical light curves measured⁹ for both GRB 041219a and GRB 990123. The black trace in **a** shows the relative (normalized to the peak value) γ -ray flux, F_γ , measured for GRB 041219a by the Swift satellite³⁰ as a function of elapsed time, $t - t_{\text{trig}}$, after recognition of the onset of a GRB at trigger time $t_{\text{trig}} = 01:42:18$ UT. The γ -ray light curve for GRB 041219a shows an outburst of precursor emission, followed by a mostly quiet period of 250 s, a primary pulse peaking at about 280 s, a secondary pulse centred at about 380 s, and finally a smaller-amplitude tertiary flux enhancement composed of minor pulses starting at 420 s after the trigger. The black trace in **b** shows the γ -ray light curve for GRB 990123, which is remarkably similar, except for a temporal scaling factor, to that measured for GRB 041219a. The relative optical fluxes, F_{opt} , are indicated by red crosses on both panels, with observing intervals denoted by horizontal red lines and 1σ flux error bars represented by red vertical lines. Together the panels show that the relationship between optical emission and γ -ray emission was quite different for the two events. Notice that the early optical flux from GRB 990123 was relatively low during the most intense γ -ray peak and only peaked in the optical⁶ after the two primary γ -ray peaks. For GRB 041219a, on the other hand, the prompt optical emission rises rapidly at the start and reaches a maximum during the primary γ -ray pulse, declines but persists during the secondary γ -ray pulse, and then fades below the detection threshold during the tertiary γ -ray enhancement. At peak brightness, GRB 041219a reached $R_c = 18.6 \pm 0.1$ mag, corresponding to an estimated peak magnitude of $R_c \approx 13.7$ after correction for extinction by dust.

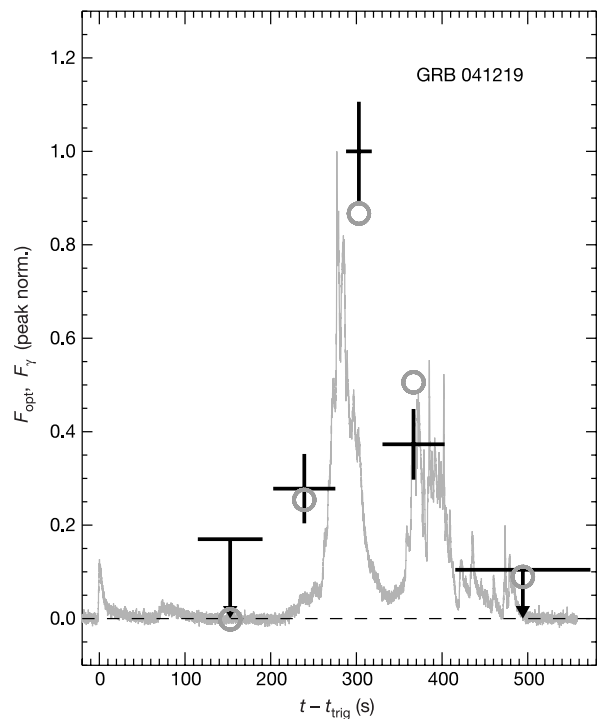


Figure 3 The measured optical light curve and that predicted for GRB 041219a assuming a constant prompt optical to prompt γ -ray flux ratio. All the optical photometry measurements are derived from stacks of two 30-s images separated by an eight-second readout time, except during the dominant γ -ray peak where a single image yielded a $>9\sigma$ detection. The γ -ray fluxes used for this comparison are derived by integrating the 15–350-keV counting rate measured by the Swift BAT, plotted as the grey trace, during the optical observation intervals. The black crosses show the actual measurements, and the circles show the predicted values. The error bars for detections are given as 1σ values, and non-detections are plotted as 2σ upper limits. The reduced χ^2 for the best-fitting model for GRB 041219a, with $F_{\text{opt}}/F_\gamma = 1.3 \times 10^{-7}$ (1.2×10^{-5} after correcting for extinction), is $\chi^2/\text{d.f.} = 1.79$ (4 degrees of freedom, d.f.). In contrast, the best-fitting model employing a constant flux ratio to predict the GRB 990123 optical light curve yields a reduced χ^2 of $\chi^2/\text{d.f.} = 1,950.65$ (2 d.f.).

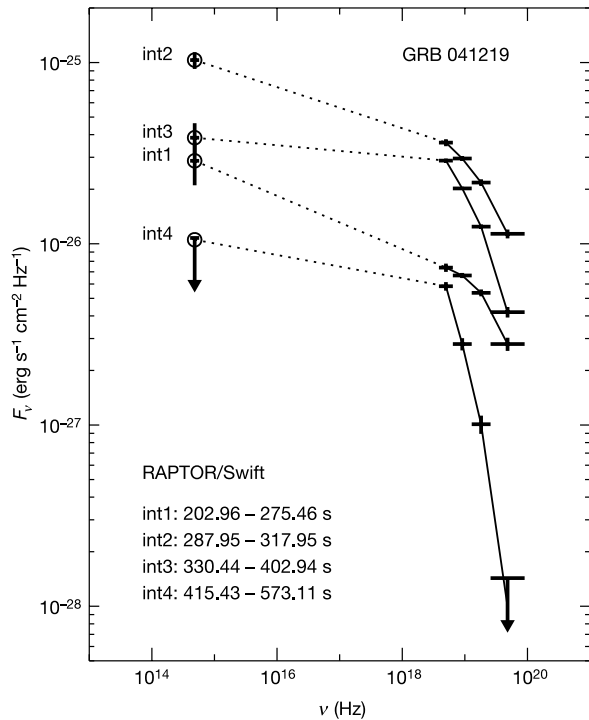


Figure 4 Broad-band spectra of GRB 041219a, here plotted in flux density F_ν , as a function of observed frequency ν , measured during the period of simultaneous prompt optical and γ -ray emission. The RAPTOR-S optical measurements, after correcting for a nominal 4.9 magnitudes of extinction, are shown as circles. Simultaneous high-energy measurements from the BAT instrument on board the Swift satellite³⁰ are shown as crosses. All the error bars represent the 1σ statistical errors. We estimate that the systematic uncertainty for the normalization of the optical fluxes is about a factor of three due to uncertainty in the intrinsic colour of the optical transient and the true extinction along the line of sight. The four integration time intervals, int1–int4, are measured in seconds from the Swift GRB trigger time at 01:42:18.7 UT on 2004 December 19. Notice the optical and γ -ray fluxes vary in concert so that the spectra never cross, and also that the highest-energy band seems to be a slightly better predictor of the behaviour of the optical emission.

the first measurement, any optical emission generated by internal shocks in GRB 990123 was outshone by bright optical emission from the external reverse shock. To generate the correlated optical and γ -ray variations measured throughout the full interval of γ -ray emission in GRB 041219a with internal (forward) shocks, reverse shock emission must be suppressed and/or delayed. The timing and strength of the reverse shock component depends strongly on the physical properties of the relativistic ejecta and the surrounding medium. In fact, the PAIRITEL near-infrared observations of GRB 041219a show the emergence of a weaker component after the end of the prompt γ -ray emission that can be interpreted as delayed reverse shock emission¹⁹.

With the addition of the new optical properties displayed by GRB 041219a to the set of known properties for optical emission from GRBs, we can construct a taxonomy of GRB optical emission with three classes: (1) prompt optical emission varying simultaneously with the prompt γ -rays; (2) early afterglow emission that may start during the prompt γ -ray emission, but persists for ten minutes or more after the prompt γ -rays have faded^{6,20–22}; and (3) late afterglow emission that can last for many hours to days^{23–25}. Within the context of the standard fireball model, it makes sense to attribute the prompt emission to internal shocks in the ultra-relativistic ejecta driven by the GRB engine², the early afterglow to a reverse

shock driven into the ejecta by interaction with the surrounding medium^{1–5,15}, and the late afterglow to forward external shocks driven into the surrounding medium generated by interaction with the ejecta^{26,27}. This theoretical framework, in turn, allows predictions about the timing, spectra and relative strength of the optical components that hinge on the properties of the inner engine, the ejecta and the surrounding medium. The ability of the Swift satellite to provide precise real-time positions and make panchromatic observations of GRBs²⁸, supplemented by a new generation of sensitive ground-based rapid response telescopes, therefore brings us into a new era in the study of the critical first few minutes during and after GRBs—one that will allow us to probe deeply the physics of these enigmatic explosions. □

Received 20 January; accepted 1 March 2005; doi:10.1038/nature03515.

1. Meszaros, P. & Rees, M. Optical and long-wavelength afterglow from gamma-ray bursts. *Astrophys. J.* **476**, 232–237 (1997).
2. Meszaros, P. & Rees, M. GRB 990123: reverse and internal shock flashes and late afterglow behaviour. *Mon. Not. R. Astron. Soc.* **306**, L39–L43 (1999).
3. Sari, R. & Piran, T. Predictions for the very early afterglow and the optical flash. *Astrophys. J.* **520**, 641–649 (1999).
4. Zhang, B., Kobayashi, S. & Meszaros, P. Gamma-ray burst early optical afterglows: Implications for the initial Lorentz factor and the central engine. *Astrophys. J.* **595**, 950–954 (2003).
5. Nakar, E. & Piran, T. Early afterglow emission from a reverse shock as a diagnostic tool for gamma-ray burst outflows. *Mon. Not. R. Astron. Soc.* **353**, 647–653 (2004).
6. Akerlof, C. *et al.* Observation of contemporaneous optical radiation from a gamma-ray burst. *Nature* **398**, 400–402 (1999).
7. Gotz, D., Mereghetti, S., Shaw, S., Beck, M. & Borkowski, J. GRB 041219 — A long GRB detected by INTEGRAL. *GRB Circ. Netw.*, 2866 (2004).
8. Barthelmy, S. *et al.* Swift-BAT detection of the bright long burst GRB 041219. *GRB Circ. Netw.*, 2874 (2004).
9. Paciesas, W. *et al.* The fourth BATSE gamma-ray burst catalog (revised). *Astrophys. J. Supp.* **122**, 465–495 (1999).
10. Vestrand, W. T. *et al.* The RAPTOR experiment: a system for monitoring the optical sky in real time. *Proc. SPIE* **4845**, 126–136 (2002).
11. Blake, C. & Bloom, J. S. GRB 041219: Infrared afterglow candidate. *GRB Circ. Netw.*, 2870 (2004).
12. Schlegel, D. J., Finkbeiner, D. P. & Davis, M. Maps of dust IR emission for use in estimation of reddening and CMBR foregrounds. *Astrophys. J.* **500**, 525–553 (1998).
13. Hearty, F. *et al.* NIR observations of GRB 041219. *GRB Circ. Netw.*, 2916 (2004).
14. Henden, A. GRB 041219, BV_{R_I} field calibration. *GRB Circ. Netw.*, 2871 (2004).
15. Panaitescu, A. & Kumar, P. Analysis of two scenarios for the early optical emission of the gamma-ray burst afterglow 990123 and 021211. *Mon. Not. R. Astron. Soc.* **353**, 511–522 (2004).
16. Kulkarni, S. R. *et al.* Discovery of a radio flare from GRB 990123. *Astrophys. J.* **522**, L97–L100 (1999).
17. Katz, J. I. Low-frequency spectra of gamma-ray bursts. *Astrophys. J.* **432**, L107–L109 (1994).
18. Liang, E. P., Crider, A., Bottcher, M. & Smith, I. A. GRB 990123: The case for saturated Comptonization. *Astrophys. J.* **519**, L21–L24 (1999).
19. Blake, C. H. *et al.* An infrared flash contemporaneous with the γ -rays from GRB 041219a. *Nature* doi:10.1038/nature03520 (this issue).
20. Vestrand, W. T. *et al.* RAPTOR: Closed-loop monitoring of the night sky and the earliest optical detection of GRB 021211. *Astron. Nachr.* **325**(6–8), 549–552 (2004).
21. Li, W., Filippenko, A., Chornock, R. & Jha, S. The early light curve of the optical afterglow of GRB 021211. *Astrophys. J.* **586**, L9–L11 (2003).
22. Fox, D. *et al.* Discovery of early optical emission from GRB 021211. *Astrophys. J.* **586**, L5–L8 (2003).
23. van Paradijs, J., Kovoveliotou, C. & Wijers, R. A. M. J. Gamma-ray burst afterglows. *Annu. Rev. Astron. Astrophys.* **38**, 379–425 (2000).
24. Stanek, K. Z. *et al.* Spectroscopic discovery of the supernova 2003dh associated with GRB 0303299. *Astrophys. J.* **591**, L17–L20 (2003).
25. Hjorth, J. *et al.* A very energetic supernova associated with the gamma-ray burst of 29 March 2003. *Nature* **423**, 847–850 (2003).
26. Waxman, E. Gamma-ray burst afterglow: supporting the cosmological fireball model, constraining parameters, and making predictions. *Astrophys. J.* **485**, L5–L8 (1997).
27. Sari, R., Piran, T. & Narayan, R. Spectra and light curves of gamma-ray burst afterglows. *Astrophys. J.* **497**, L17–L20 (1998).
28. Gehrels, N. *et al.* The Swift gamma-ray burst mission. *Astrophys. J.* **611**, 1005–1020 (2004).
29. Cenko, S. B. GRB 041219: optical afterglow detection. *GRB Circ. Netw.* 2886 (2004).
30. Fenimore, E. *et al.* Swift-BAT time history of GRB 041219. *GRB Circ. Netw.* 2906 (2004).

Supplementary Information accompanies the paper on www.nature.com/nature.

Acknowledgements The RAPTOR project is supported by the Laboratory Directed Research and Development programme at Los Alamos National Laboratory.

Competing interests statement The authors declare that they have no competing financial interests.

Correspondence and requests for materials should be addressed to W.T.V. (vestrand@lanl.gov).